



Graphene-based field effect transistor in two-dimensional paper networks



Aldrine Abenoja Cagang^a, Irfan Haider Abidi^a, Abhishek Tyagi^a, Jie Hu^{b,c}, Feng Xu^{b,c}, Tian Jian Lu^b, Zhengtang Luo^{a,*}

^a Department of Chemical and Biomolecular Engineering, Hong Kong University of Science and Technology, Clear Water Bay, Hong Kong

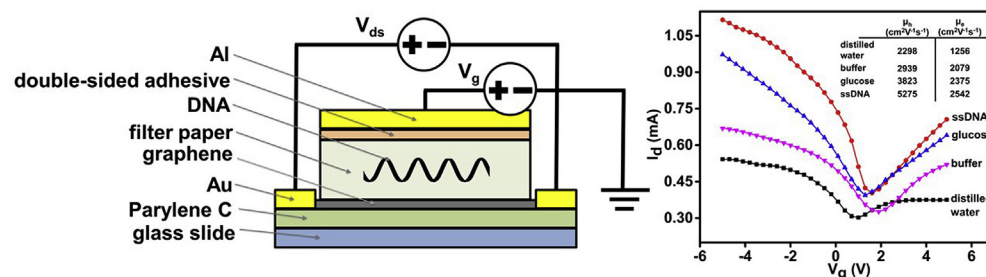
^b Bioinspired Engineering and Biomechanics Center (BEBC), Xi'an Jiaotong University, Xi'an 710049, PR China

^c The Key Laboratory of Biomedical Information Engineering of Ministry of Education, School of Life Science and Technology, Xi'an Jiaotong University, Xi'an 710049, PR China

HIGHLIGHTS

- A graphene-based field effect transistor sensor was fabricated for two-dimensional paper network formats.
- The constructed GFET on 2DPN was shown to behave similarly to solution-gated GFETs.
- Electrolyte gating effects have more prominent effect over adsorption effects on the behavior of the device.
- The GFET incorporated on 2DPN was shown to yield linear response to presence of glucose and ssDNA soaked inside the paper.

GRAPHICAL ABSTRACT



ARTICLE INFO

Article history:

Received 15 December 2015

Received in revised form

26 February 2016

Accepted 1 March 2016

Available online 5 March 2016

Keywords:

Graphene field effect transistors
Paper analytical devices
Two-dimensional paper networks
Paper microfluidics

ABSTRACT

We demonstrate the fabrication of a graphene-based field effect transistor (GFET) incorporated in a two-dimensional paper network format (2DPNs). Paper serves as both a gate dielectric and an easy-to-fabricate vessel for holding the solution with the target molecules in question. The choice of paper enables a simpler alternative approach to the construction of a GFET device. The fabricated device is shown to behave similarly to a solution-gated GFET device with electron and hole mobilities of $\sim 1256 \text{ cm}^2 \text{ V}^{-1} \text{ s}^{-1}$ and $\sim 2298 \text{ cm}^2 \text{ V}^{-1} \text{ s}^{-1}$ respectively and a Dirac point around $\sim 1 \text{ V}$. When using solutions of ssDNA and glucose it was found that the added molecules induce negative electrolytic gating effects shifting the conductance minimum to the right, concurrent with increasing carrier concentrations which results to an observed increase in current response correlated to the concentration of the solution used.

© 2016 Elsevier B.V. All rights reserved.

1. Introduction

Paper is a well-known material with abundant utilities not only

in writing, printing and packaging, but also in traditional laboratory techniques such as filtration and paper chromatography. Recently, paper is being rediscovered as a material for many different areas of research like electronics and biomedical applications. The upsurge in attention is due to some advantageous properties that are inherent to paper such as porosity, flexibility and capillary flow in

* Corresponding author.

E-mail address: keztluo@ust.hk (Z. Luo).

addition to its ease of manipulation and low-cost. One of the developing areas of research interest for paper is two-dimensional paper networks (2DPNs) otherwise also known as paper microfluidics. 2DPNs were shown to be comparable to the conventional continuous-flow microfluidics exhibiting the same characteristic laminar flow processes. However, the paper-based microfluidic counterpart does not need any external pumps because of capillary flow and is far easier to fabricate. And in many recent research progress, a number of the capabilities of continuous-flow microfluidics have been translated into its paper format. It was demonstrated that patterns can be placed on paper to create channels for directed fluid flow which offered advantages of multiplexed analysis from a single sample introduction transcending the capabilities of sensing seen from the traditional lateral flow assays (LFAs) [1–3]. In addition, the same idea and principle was employed to carry out multi-step processes by linking multiple inlets to a shared region and precise control of flow is also shown to perform sequential steps [4,5].

In most 2DPNs the applications are geared toward sensing biomolecules such as DNA [6], proteins [7] or certain metabolites and infectious diseases [8] mainly through qualitative colorimetric detection [9] or quantitative electrochemical detection [10]. In this report, we demonstrate the incorporation of a Field Effect Transistor (FET) type sensor onto a paper platform with the use of graphene as a channel. Graphene, a two-dimensional sheet of sp^2 hybridized carbon, has also gathered research attention in sensing applications owing to its good electronic properties particularly its ultra-high mobility and ambipolar field effect in addition to the very large surface area of its two-dimensional structure. With advances in large-scale synthesis through chemical vapor deposition (CVD) techniques, a great number of reports have utilized graphene as a sensing platform in particular as an FET. The exceptional electronic properties of graphene has great potential for sensing and paves a way for better precision and accuracy which are important in sensing tools especially in applications like medical diagnostics [11]. At present there are still challenges towards the achievement of precise and accurate measurements even with the significant improvements in many sensing systems. For example, many sensing tools rely on the measurement of hydrogen peroxide produced from the reaction of an analyte with its appropriate oxidase enzyme. It is an indirect measurement and is subject to many interferences from other electroactive species [12]. Graphene-based field effect transistors (GFETs) offer the advantage over other sensing approaches such as optical and electrochemical detection in that it is feasible to perform label-free detection with good sensitivity [13]. In fact, GFETs have been employed to detect DNA and its hybridization and other biomolecules by monitoring conductivity changes [14–16]. In addition, GFET has been reported to be incorporated as a sensor in continuous-flow microfluidics [17]. GFETs by itself has recently been shown to have versatile qualities by being incorporated in various formats especially in flexible substrates owing to the graphene material being also flexible [18]. In this regard, our report will help transcend the capabilities of 2DPNs and further translate processes carried out in continuous-flow microfluidics into its paper format by incorporating paper as a dielectric material for a GFET. There is a considerable amount of research aimed at simplifying sensing platforms without compromising performance in sensitivity and accuracy. Graphene has enabled the further development of paper sensing platforms for highly sensitive and rapid detection of analytes [19].

2. Experimental details

2.1. Preparation of graphene film by chemical vapor deposition (CVD)

The graphene sheets used in this study were synthesized via chemical vapor deposition (CVD) [20,21]. More specifically, a piece of copper foil was shortly etched for 30 s in a $FeCl_3$ solution with mild sonication followed by blow-drying using a nitrogen gun. The foil was then placed inside the CVD furnace where it was treated with Ar gas flowing at 30 sccm for 20 min and then annealed by adding H_2 gas flowing at 16 sccm to a temperature of 1050 °C. Graphene was grown by introducing CH_4 gas into the furnace as a carbon source at 16 sccm for 20 min while maintaining the flow of Ar and H_2 .

2.2. Fabrication of graphene-based field effect transistor (GFET)

The prepared graphene was subsequently transferred onto a glass slide precoated with 1 μm Parylene C. The transfer process involves spin-coating a layer of PMMA solution on the side of the copper foil with graphene and then baking the PMMA to dry at 120 °C. Keeping the PMMA side face up, the underside copper was etched by floating the foil in a $FeCl_3$ solution for 5 h. After the copper is completely etched, graphene attached to PMMA was carefully scooped out using a glass slide and floated back on a dilute HCl solution and then DI water each for 1 h. Finally, the graphene is scooped into the desired Parylene-coated glass slide after which the PMMA layer was removed by bathing the slide in acetone for 5 min at 60 °C.

The construction of the FET device was done by forming 50 nm gold contacts on two ends of the graphene sheet via thin film sputtering. A Whatman Grade No. 1 filter paper was manually cut into small pieces, which was then stuck with a sheet of aluminum foil using a double-sided adhesive. The paper was soaked with the solution in question (e.g. glucose solution and ssDNA solution) and then carefully positioned on top of the graphene sheet. A schematic illustration and an image of the actual device are shown in Fig. 1a. The ssDNA used as a model analyte was an oligonucleotide for HIV-1 detection with a sequence 5'-AGTAGTGTGTCGCCGTCTGTTGTGACTCTGTAAGTACTAGATCCCTCAGAC-3' [6].

2.3. Characterization

Raman spectroscopy of graphene was done using an InVia Renishaw Raman Microscope with a 514 nm excitation Argon laser. AFM images were obtained using a Veeco Multimode Scanning Probe Microscope. Device electrical characterization was carried out using a Signatone S-1160B Manual Probe Station.

3. Results and discussion

Our approach to incorporating a GFET device onto a 2DPN is to use a solution-soaked paper as a gate dielectric material for the device. Fig. 1a illustrates the configuration of the GFET as explained in the experimental section. Graphene is constructed as a channel between two contacts, and its current can be modulated by application of an electric field through a gate electrode on top. Paper with absorbed solutions serves a dielectric material in between the channel and gate where charged species from the solution can contribute to the field effect. Parylene C was coated on the surface of the glass slide to provide a hydrophobic surface for better graphene adhesion. Gold serves as good ohmic contacts for electronic characterization and is resistant to oxidation. For the gate electrode, sputtering gold on top of the filter paper was found to not be an

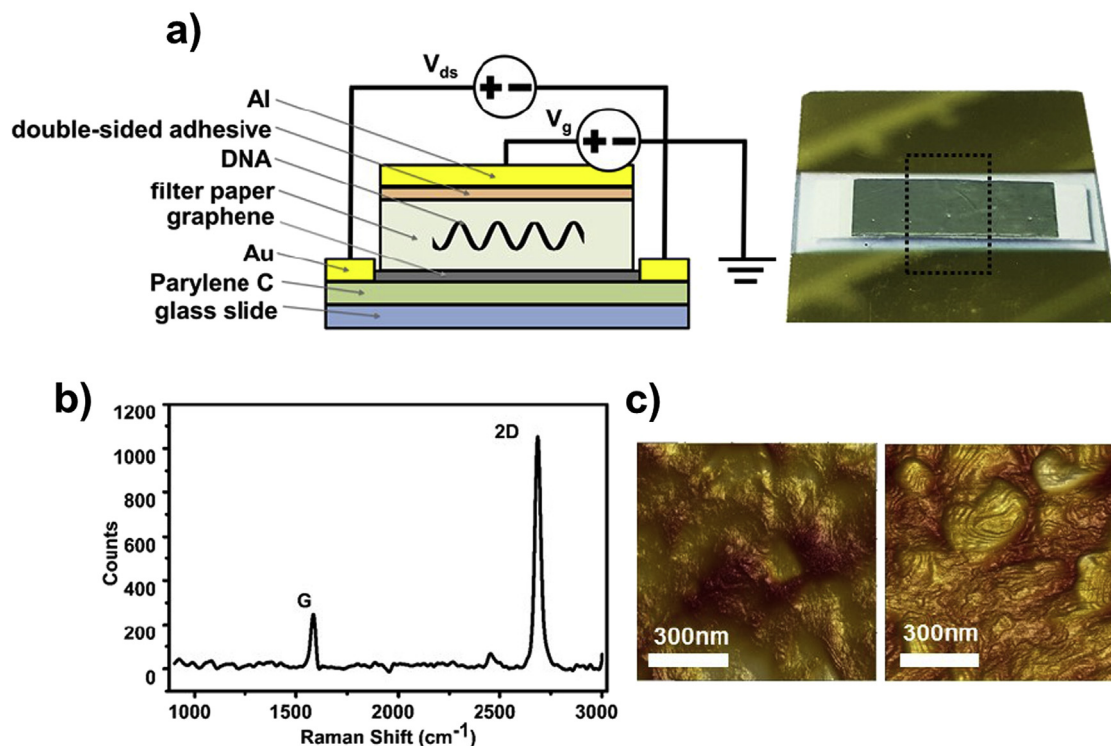


Fig. 1. (a) Cross sectional schematic illustration of the GFET device and image of the actual device. Graphene sheet is outlined. (b) Raman spectrum of the transferred graphene sheet. The spectrum of the underlying Parylene C layer have been subtracted. (c) AFM image showing the Parylene surface before (left) and after (after) graphene transfer.

ideal procedure as gold would absorb into and penetrate through the porous structure of the paper [22] leaving no more room for the sample to soak into. Sticking aluminum foil via double-sided adhesive was used instead, which favorably provided a simpler and low-cost alternative to the fabrication. The high quality of the graphene produced from our method is confirmed with Raman spectroscopy, as shown in Fig. 1b. Since the graphene sheet was deposited onto a Parylene-coated surface, the spectrum initially depicts several peaks instead of the typical G and 2D peaks prominent for graphene [23], however, subtracting the spectrum of a bare Parylene C surface made apparent the characteristic G and 2D peaks observed around $\sim 1583 \text{ cm}^{-1}$ and $\sim 2692 \text{ cm}^{-1}$ respectively. The G peak is very small relative to a sharp and symmetrical 2D peak with a 2D/G peak ratio ~ 3 , consistent with the reported Raman spectra of monolayer of graphene [24–26]. This is corroborated with AFM indicating a step height of $\sim 1\text{--}2 \text{ nm}$ at the edges. Fig. 1c shows the AFM image taken at the center part of the sheet of the transferred graphene (right) and the bare Parylene C surface (left). The image suggests that the graphene is continuous with only the wrinkles indicating its presence typical of a transferred CVD graphene [27].

To confirm the electronic properties of the graphene devices, we studied the current-gate voltage ($I\text{--}V_g$) characteristics as shown in Fig. 2a using V_{ds} at 1 V with the current-drain voltage ($I\text{--}V_d$) curve depicted in the inset. From the inset, we can see the increase in drain current upon application of bias to the gate voltage. This is corroborated by the characteristic $I\text{--}V_g$ curve, which shows an ambipolar behavior response typical for graphene-based FETs [28]. It is a crucial note that in order for the paper GFET to function properly the paper must be soaked with liquid which in this initial case was distilled water. The conductance minimum (Dirac point) of the characteristic curve is found around $\sim 1 \text{ V}$ which is comparable to those of conventional solution-gated GFET configurations [29–31] with its slight shift to the positive voltage attributed to

defects and p-doping [32]. Considering the thickness of the paper, it is expected to demonstrate conductance minimum at higher positive potentials comparable to back-gated GFET configurations [33]; however, the characteristic curve indicates a gating mechanism similar to solution-gated GFETs. The carrier mobilities were extracted from the slope of the linear regime of the characteristic curve, which gives the device transconductance. The transconductance is defined by the equation $g_m = (W/L)\mu C_0 V_{ds}$ where g_m is the transconductance, (W/L) is the width to length ratio of the channel, μ is the carrier mobility, C_0 is the specific capacitance between the gate and channel and V_{ds} is the supplied drain-source voltage [34]. The (W/L) and V_{ds} are given numbers with values of 0.7 and 1 V respectively. The C_0 was measured using an LCR meter which provided a range of values near $\sim 54 \text{ nFcm}^{-2}$. The electron and hole mobilities were solved to have values of ~ 1256 and $\sim 2298 \text{ cm}^2 \text{ V}^{-1} \text{ s}^{-1}$ respectively which are typical values for GFETs [33,34] although comparatively lesser than conventionally structured GFETs using traditional dielectric materials between the gate electrode [35,36].

We investigated the $I\text{--}V_g$ characteristic as a function of the nature of analytes and their concentration. Fig. 2b shows the characteristic curve of the device using 25 nM ssDNA, which yielded higher current responses when negatively or positively biased in the gate in comparison with only DI water soaking the paper between the channel and the gate suggesting an effect of solute or ions present similar to solution-gated FETs [37,38]. The slight increase in current response with buffer solution is also attributed to this due to the presence of ions in solution. In addition increasing the V_{ds} slightly shifts the Dirac point towards more positive gate voltages. The position of the Dirac point is a result of factors that involve the difference in work functions between the graphene and gate electrode, the type and density of charges at the interfaces at the top and bottom of the channel and any doping effects on graphene [32]. The increase in current response with the presence of

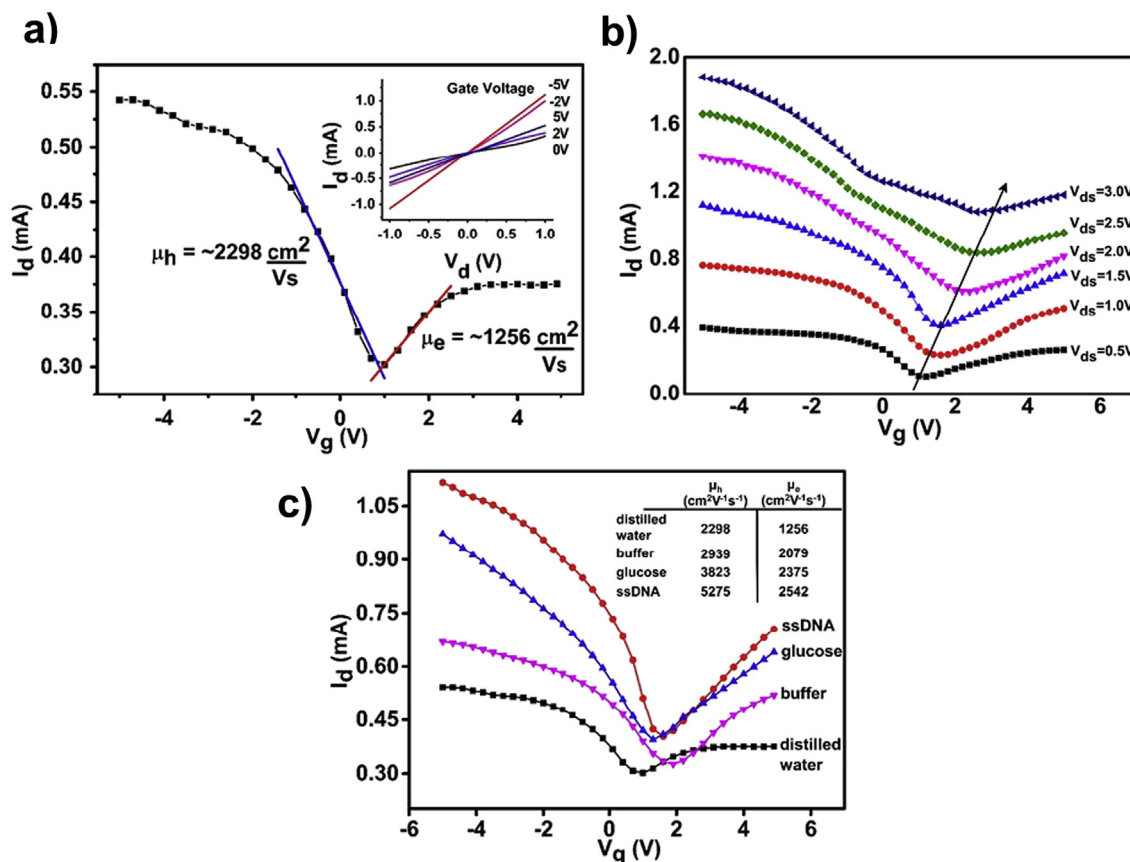


Fig. 2. (a) Characteristic curve of the fabricated GFET using distilled water as liquid medium with corresponding carrier mobilities at $V_{ds} = 1$ V. Inset shows the output response curves at various gate voltages. (b) Characteristic curve of the GFET device using 25 nM ssDNA at various drain-source voltages. (c) Characteristic curves using different liquids soaking the filter paper with corresponding mobilities.

ssDNA implies increase in transconductance in consequence with increase in carrier mobility associated with the increase in the interfacial capacitance between the graphene and the gate [39]. It has been reported that the interaction of ssDNA with graphene would expectedly decrease its carrier mobility due to defects brought about by adsorption and immobilization of ssDNA onto the surface of graphene. In addition, the prominent interaction of nucleobases of ssDNA would induce a left shift of the Dirac point [40]. Fig. 2c shows that in this case, the presence of ssDNA shifts the Dirac point to the right and increases the mobility instead. This suggests that electrostatic gating effects coming from the negative charges of ssDNA are more prominent than adsorption effects coming from the interaction of ssDNA with graphene. The ssDNA mainly induces increase in capacitance between the graphene and gate. The right shift can be attributed to the fact that ssDNA is typically negatively charged because of its phosphate backbone and its presence would require more positive gate voltages to screen it off [40]. A similar behavior in the characteristic curve is seen with glucose solutions. The hexagonal ring structure of glucose enables stacking and adsorption of its molecules with graphene which in turn facilitates charge transfer from glucose to graphene [41]. The transfer curves at different concentrations of ssDNA and glucose are depicted in Fig. 3a and Fig. 3b respectively which exhibit the same right shift of the conductance minimum attributed to the additional negative gating effect of the molecules. Specific capacitances were measured for the soaked solutions which results to a corresponding increase in charge carriers as indicated in their respective insets. The number of charge carriers were obtained using the specific capacitances following the equation $n = (1/q)C_o(V_g - V_{dirac})$ where n

is the carrier concentration, q is the elemental charge, C_o is the specific capacitance, V_g is the applied gate voltage and V_{dirac} is the conductance minimum extracted from the characteristic curves [42]. However, it is observed that the addition of increasing concentrations of ssDNA soaked within the paper structure produces a contrary trend in their transfer curves where it can be seen that the linear regime both for hole and electron transport are becoming less steep. This translates to a decrease in carrier mobilities. Increase in electrolyte gating from the presence of charged species typically induces accumulation of more carriers, hence the increase in its density. Doping effects from the interaction of species with the graphene sheet have been shown to not significantly affect the mobilities [43], however, several reports have noted the same observation of mobility decrease with carrier density increase attributing it to additional Coulomb scattering due to the double layer formed at the graphene-solution interface [44]. The increase in ion density at the graphene interface with the presence of more charged ssDNA species correspondingly introduces more ionic scattering centers, hence the observed decrease in carrier mobility.

The key feature of the described GFET is the soaked filter paper between the gate electrode and graphene sheet, which can be taken advantage of by introducing different solutions appropriate for sensing applications acting as an easily fabricated vessel. The shape of the characteristic curve specifically for the model analytes used (ssDNA and glucose) implies operation with a negative bias on the gate to yield higher change in current response. Fig. 4a and Fig. 4b show chronoamperograms of the device using different concentrations of ssDNA and glucose demonstrating increase of current response attributed to the presence of the analytes. The

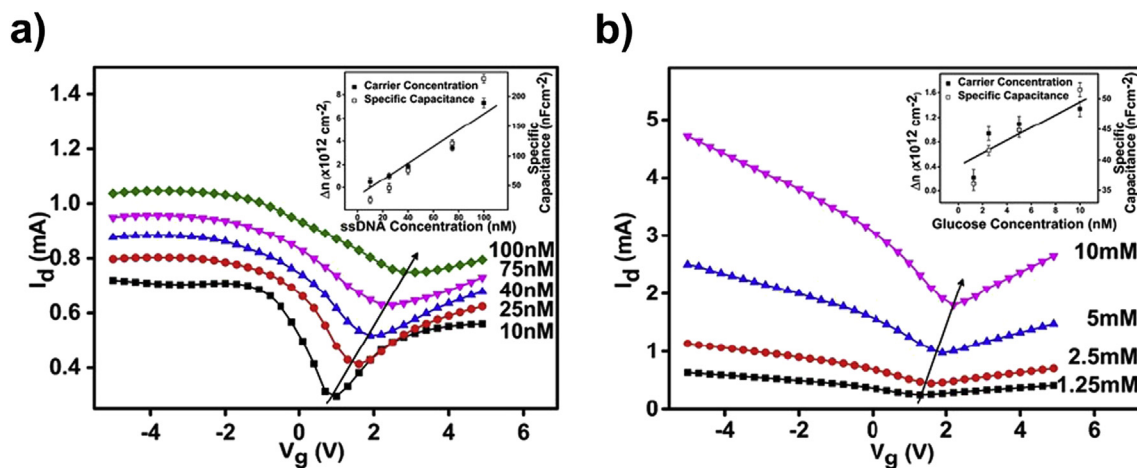


Fig. 3. Characteristic curves using different concentrations soaking the filter paper of (a) ssDNA and (b) glucose. Injected carrier concentrations and measured specific capacitance shown as insets.

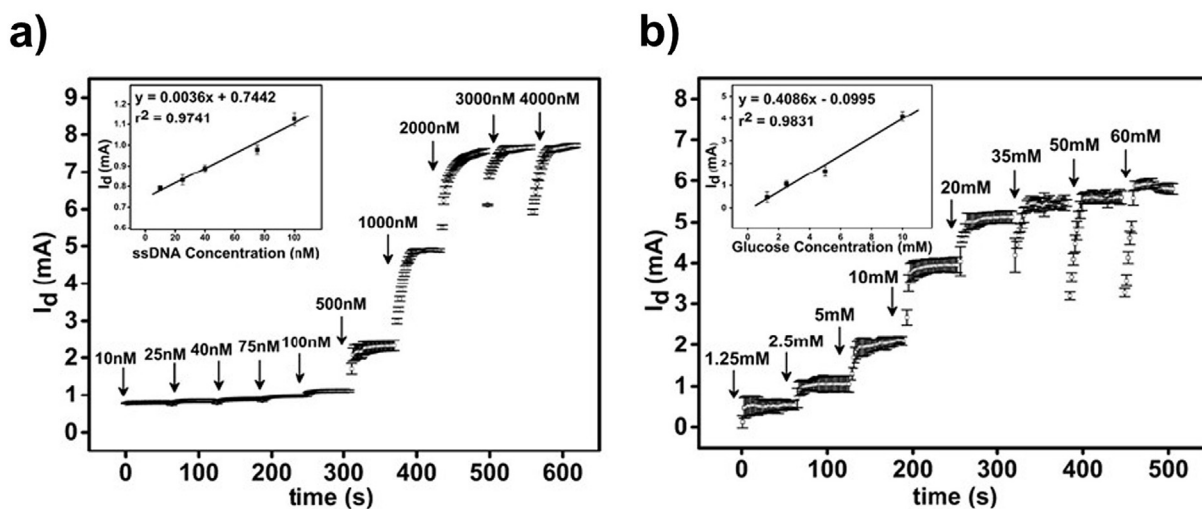


Fig. 4. Chronoamperometry of GFET device using various concentrations and the corresponding calibration curves shown as insets of (a) ssDNA and (b) glucose.

analytes ssDNA and glucose were selected, as these are targets prominent to many biomedical sensing and POC applications. The ssDNA used as a model analyte was an oligonucleotide for HIV-1 detection. Chronoamperometry samples the current of the device over time, which provides a more precise measurement [45] as suggested with the stable current responses. As shown in the respective insets within the figures, the device is able to provide a linear calibration curve at the relevant range of concentration of the selected analytes and can go as low as 10 nM for the ssDNA and 1.25 mM for glucose. The sensitivity can be extracted from the slope of the calibration curves, which yielded $0.0036 \text{ mA nM}^{-1}$ and $0.4086 \text{ mA mM}^{-1}$ for ssDNA and glucose respectively. Further optimization of the device by operating at higher V_{ds} or using more negative gate voltages can improve the sensitivity. The chronoamperograms depict an onset of saturation at around 2000 nM for ssDNA and 35 mM for glucose.

4. Conclusion

This study demonstrates the use of a wet filter paper as a dielectric material for a graphene-based FET device. The use of paper as a dielectric material was achieved by soaking the paper

with liquid medium, which can be used to detect presence of clinically pertinent molecules such as glucose and ssDNA. The constructed GFET was shown to have electron and hole mobilities at around $\sim 1256 \text{ cm}^2 \text{ V}^{-1} \text{ s}^{-1}$ and $\sim 2298 \text{ cm}^2 \text{ V}^{-1} \text{ s}^{-1}$ respectively. Introduction of ssDNA and glucose into the paper matrix increases the specific capacitance between the top gate and graphene channel which applies gating effects correlated with the analyte's concentration. The behavior of the resulting characteristic curves of the device exhibits similarity to solution-gated GFETs; however negative electrolyte gating effects were more prominent over adsorption interactions and doping effects between graphene and the ssDNA and glucose molecules. The filter paper used for the GFET provides an easily fabricated vessel for the medium to be questioned using its absorbent properties and widens the capabilities of 2DPNs for various applications such as analytical devices.

Acknowledgment

This project is supported by the Research Grant Council of Hong Kong SAR (Project number 16204815) and SFC/RGC Joint Research Scheme (Project number X-HKUST603/14). J.H., F.X. and T.J.L. were financially supported by the Major International Joint Research

Program of China (11120101002). Technical assistance from the Materials Characterization and Preparation Facilities is greatly appreciated.

References

- [1] A.W. Martinez, S.T. Phillips, M.J. Butte, G.M. Whitesides, Patterned paper as a platform for inexpensive, low-volume, portable bioassays, *Angew. Chem. Int. Ed.* 46 (2007) 1318–1320.
- [2] S.T. Sanjay, G. Fu, M. Dou, F. Xu, R. Liu, H. Qi, X. Li, Biomarker detection for disease diagnosis using cost-effective microfluidic platforms, *Analyst* 140 (2015) 7062–7081.
- [3] M. Dou, S.T. Sanjay, M. Benhabib, F. Xu, X. Li, Low-cost bioanalysis on paper-based and its hybrid microfluidic platforms, *Talanta* 145 (2015) 43–54.
- [4] E.M. Fenton, M.R. Mascarenas, G.P. Lopez, S.S. Sibbett, Multiplex lateral-flow test strips fabricated by two-dimensional shaping, *ACS Appl. Mater. Interfaces* 1 (2009) 124–129.
- [5] E. Fu, B. Lutz, P. Kauffman, P. Yager, Controlled reagent transport in disposable 2D paper networks, *Lab. Chip* 10 (2010) 918–920.
- [6] J. Hu, L. Wang, F. Li, Y.L. Han, M. Lin, T.J. Lu, F. Xu, Oligonucleotide-linked gold nanoparticle aggregates for enhanced sensitivity in lateral flow assays, *Lab. Chip* 13 (2013) 4352–4357.
- [7] K. Yamada, T.G. Henares, K. Suzuki, D. Citterio, Distance-based tear lactoferrin assay on microfluidic paper device using interfacial interactions on surface-modified cellulose, *ACS Appl. Mater. Interfaces* 7 (2015) 24864–24875.
- [8] M. Dou, D.C. Dominguez, X. Li, J. Sanchez, G. Scott, A versatile PDMS/paper hybrid microfluidic platform for sensitive infectious disease diagnosis, *Anal. Chem.* 86 (2014) 7978–7986.
- [9] E. Carrilho, S.T. Phillips, S.J. Vella, A.W. Martinez, G.M. Whitesides, Paper microzone plates, *Anal. Chem.* 81 (2009) 5990–5998.
- [10] Z. Nie, C.A. Nijhuis, J. Gong, X. Chen, A. Kumachev, A.W. Martinez, M. Narovlyansky, G.M. Whitesides, Electrochemical sensing in paper-based microfluidic devices, *Lab Chip* 10 (2010) 477–483.
- [11] S. Viswanathan, T.N. Narayanan, K. Aran, K.D. Fink, J. Paredes, P.M. Ajayan, S. Filipek, P. Miszta, H.C. Tekin, F. Inci, U. Demirci, P. Li, K.I. Bolotin, D. Liepmann, V. Renugopalakrishnan, Graphene-protein field effect biosensors: glucose sensing, *Mater. Today* 18 (2015) 513.
- [12] J. S. Krouwer, G. S. Cembrowski, A review of standards and statistics used to describe blood glucose monitor performance *J. Diabetes. Sci. Technol.*, 4 (2010) 75–83.
- [13] K.S. Novoselov, A.K. Geim, S.V. Morozov, D. Jiang, Y. Zhang, S.V. Dubonos, I.V. Grigorieva, A.A. Firsov, Electric field effect in atomically thin carbon films, *Science* 306 (2004) 666–669.
- [14] R. Stine, J.T. Robinson, P.E. Sheehan, C.R. Tamanaha, Real-time DNA detection using reduced graphene oxide field effect transistors, *Adv. Mater.* 22 (2010) 5297–5300.
- [15] S. Mao, G. Lu, K. Yu, Z. Bo, J. Chen, Specific protein detection using thermally reduced graphene oxide sheet decorated with gold nanoparticle-antibody conjugates, *Adv. Mater.* 22 (2010) 3521–3526.
- [16] Y.H. Kwak, D.S. Choi, Y.N. Kim, H. Kim, D.H. Yoon, S.S. Ahn, J.W. Yang, W.S. Yang, S. Seo, Flexible glucose sensor using CVD-grown graphene-based field effect transistor, *Biosens. Bioelectron.* 37 (2012) 82–87.
- [17] P.K. Ang, A. Li, M. Jaiswal, Y. Wang, H.H. Hou, J.T.L. Thong, C.T. Lim, K.P. Loh, Flow sensing of single cell by graphene transistor in a microfluidic channel, *Nano Lett.* 11 (2011) 5240–5246.
- [18] T.Q. Trung, N.T. Tien, D. Kim, M. Jang, O.J. Yoon, N.E. Lee, A flexible reduced graphene oxide field-effect transistor for ultrasensitive strain sensing, *Adv. Funct. Mater.* 24 (2014) 117–124.
- [19] P. Labroo, Y. Cui, Graphene nano-ink biosensor arrays on a microfluidic paper for multiplexed detection of metabolites, *Anal. Chim. Acta* 813 (2014) 90–96.
- [20] L. Gan, H. Zhang, R. Wu, Y. Ding, P. Sheng, Z. Luo, Controlled removal of monolayers for bilayer graphene preparation and visualization, *RSC Adv.* 5 (2015) 25471–25476.
- [21] L. Gan, X. Ou, Q. Zhang, R. Wu, Z. Luo, Graphene amplification by continued growth on seed edges, *Chem. Mater.* 26 (2014) 4137–4143.
- [22] A.C. Siegel, S.T. Phillips, M.D. Dickey, N. Lu, Z. Suo, G.M. Whitesides, Foldable printed circuit boards on paper substrates, *Adv. Funct. Mater.* 20 (2010) 28–35.
- [23] M.A. Pimenta, G. Dresselhaus, M.S. Dresselhaus, L.G. Cancado, A. Jorio, R. Saito, Studying disorder in graphite-based systems by Raman spectroscopy, *Phys. Chem. Chem. Phys.* 9 (2007) 1276–1291.
- [24] A. Inaba, K. Yoo, Y. Takei, K. Matsumoto, I. Shimoyama, Ammonia gas sensing using a graphene field-effect transistor gated by ionic liquid, *Sens. Actuat. B-Chem.* 195 (2014) 15–21.
- [25] Z. Ni, Y. Wang, T. Yu, Z. Shen, Raman spectroscopy and imaging of graphene, *Nano Res.* 1 (2008) 273–291.
- [26] A. Gupta, G. Chen, P. Joshi, S. Tadigadapa, P.C. Eklund, Raman scattering from high-frequency phonons in supported n-graphene layer films, *Nano Lett.* 6 (2006) 2667.
- [27] W. Zhu, T. Low, V. Perebeinos, A.A. Bol, Y. Zhu, H. Yan, J. Tersoff, P. Avouris, Structure and electronic transport in graphene wrinkles, *Nano Lett.* 12 (2012) 3431–3436.
- [28] I. Meric, M.Y. Han, A.F. Young, B. Ozyilmaz, P. Kim, K.L. Shepard, Current saturation in zero-bandgap, top-gated graphene field-effect transistors, *Nat. Nanotechnol.* 3 (2008) 654.
- [29] X. Dong, Y. Shi, W. Huang, P. Chen, L.J. Li, Electrical detection of dna hybridization with single-base specificity using transistors based on CVD-grown graphene sheets, *Adv. Mater.* 22 (2010) 1649–1653.
- [30] F. Chen, Q. Qing, J. Xia, J. Li, N. Tao, Electrochemical gate-controlled charge transport in graphene in ionic liquid and aqueous solution, *J. Am. Chem. Soc.* 131 (2009) 9908–9909.
- [31] Z. Yin, Q. He, X. Huang, J. Zhang, S. Wu, P. Chen, G. Lu, P. Chen, Q. Zhang, Q. Yan, H. Zhang, Real-time DNA detection using Pt nanoparticle-decorated reduced graphene oxide field-effect transistors, *Nanoscale* 4 (2012) 293.
- [32] F. Schwierz, Graphene transistors, *Nat. Nanotechnol.* 5 (2010) 487.
- [33] Y. Lee, S. Bae, H. Jang, S. Jang, S.E. Zhu, S.H. Sim, Y.I. Song, B.H. Hong, J.H. Ahn, Wafer-scale synthesis and transfer of graphene films, *Nano Lett.* 10 (2010) 490–493.
- [34] B.J. Kim, H. Jang, S.K. Lee, B.H. Hong, J.H. Ahn, J.H. Cho, High-performance flexible graphene field effect transistors with ion gel gate dielectrics, *Nano Lett.* 10 (2010) 3464–3466.
- [35] Y. Lu, B.R. Goldsmith, N.J. Kybert, A.T.C. Johnson, DNA-decorated graphene chemical sensors, *Appl. Phys. Lett.* 97 (2010) 083107.
- [36] Y. Dan, Y. Lu, N.J. Kybert, Z. Luo, A.T.C. Johnson, Intrinsic response of graphene vapor sensors, *Nano Lett.* 9 (2009) 1472–1475.
- [37] Y. Ohno, K. Maehashi, Y. Yamashiro, K. Matsumoto, Electrolyte-gated graphene field-effect transistors for detecting pH and protein adsorption, *Nano Lett.* 9 (2009) 3318–3322.
- [38] M. Dankerl, M.V. Hauf, A. Lippert, L.H. Hess, S. Birner, I.D. Sharp, A. Mahmood, P. Mallet, J.Y. Veuillen, M. Stutzmann, J.A. Garrido, Graphene solution-gated field effect transistor array for sensing applications, *Adv. Funct. Mater.* 20 (2010) 3117–3124.
- [39] L.H. Hess, M.V. Hauf, M. Seifert, F. Speck, T. Seyller, M. Stutzmann, I.D. Sharp, High-transconductance graphene solution-gated field effect transistors, *Appl. Phys. Lett.* 99 (2011) 033503.
- [40] C.T. Lin, P.T.K. Loan, T.Y. Chen, K.K. Liu, C.H. Chen, K.H. Wei, L.J. Li, Label-free electrical detection of DNA hybridization on graphene using hall effect measurements: revisiting the sensing mechanism, *Adv. Funct. Mater.* 23 (2013) 2301–2307.
- [41] S. Chattopadhyay, M.S. Li, P.K. Roy, C.T. Wu, Non-enzymatic glucose sensing by enhanced Raman spectroscopy on flexible 'as-grown' CVD graphene, *Analyst* 140 (2015) 3935–3941.
- [42] Z. Zhang, H. Xu, H. Zhong, L.M. Peng, Direct extraction of carrier mobility in graphene field-effect transistor using current-voltage and capacitance-voltage measurements, *Appl. Phys. Lett.* 101 (2012) 213103.
- [43] F. Schedin, A.K. Geim, S.V. Morozov, E.W. Hill, P. Blake, M.I. Katsnelson, K.S. Novoselov, Detection of individual gas molecules adsorbed on graphene, *Nat. Mater.* 6 (2007) 652.
- [44] J.L. Tedesco, B.L. VanMil, R.L. Myers-Ward, J.M. McCrate, S.A. Kitt, P.M. Campbell, G.G. Jernigan, J.C. Culbertson, C.R. Eddy Jr., D.K. Gaskill, Hall effect mobility of epitaxial graphene grown on silicon carbide, *Appl. Phys. Lett.* 95 (2009) 122102.
- [45] W. Dungchai, O. Chailapakul, C.S. Henry, Electrochemical detection for paper-based microfluidics, *Anal. Chem.* 81 (2009) 5821–5826.